

## Reference-free Coating Thickness Quantification using Laser Thermography under Various Exterior Temperature Conditions

by S. Hwang\*, J. Park\*, Z. Jin\* and H. Sohn\*

\* Department of Civil and Environmental Engineering, KAIST, 291 Daehak-ro, Daejeon 34141, South Korea, [hoonsohn@kaist.ac.kr](mailto:hoonsohn@kaist.ac.kr)

### Abstract

This paper presents a reference-free paint-thickness visualization method using thermography. When thermal-waves generated by a continuous-wave laser are applied to a paint-surface, the thermal-waves propagate through the paint-layer and the resultant thermal-waves are measured by an infrared camera. The propagating characteristics of thermal-waves through the paint-layer are altered from the changes on the thickness of paint-layer. Accordingly, the alternation can be mapped as the paint-thickness regardless of varying exterior temperature conditions by analysing the phase and amplitude of the thermal-waves acquired by the infrared camera, and the accuracy of the thickness quantification can be further enhanced by additional image processes.

### 1. Introduction

A paint layer is essential for the metallic structure and widely used throughout the industry to protect the metallic structures from the various exterior conditions such as humidity, direct sunlight, and salty conditions [1-3]. An improper paint thickness can cause the corrosion and section loss of the metallic structures [4, 5], and the local damage on the metallic structures can cause a stress concentration, and accelerate the structural deterioration [6, 7]. For example, several bridges were collapsed by poor quality control of paint layer, e.g. section loss from corrosion on I35W Bridge and Silver Bridge in US [8-10]. Thus, the paint thickness management is gaining its importance, and the regulations and guidelines for paint thickness management are continuously establishing.

A number of non-destructive techniques (NDT) are proposed to measure the paint thickness. The most widely used NDT technique is an eddy current technique which can predict the paint thickness by measuring the changes in magnetic fields due to the paint thickness variations [11, 12]. The eddy current technique can measure the paint thickness with low power consumption and cheap instruments within short inspection time. However, the equipment must be attached to the target structure to perform the paint thickness inspection. The ultrasonic techniques are also used to inspect the paint thickness by measuring the time delay and velocity of ultrasonic waves in the paint layers [13, 14]. The ultrasonic technique is gaining its strength since it can measure the thickness of the multiple paint layers. However, the couplant must be applied between the target structure and the sensor to perform the inspection with ultrasonic technique. To tackle the problems arising from the contact inspection mechanism, a terahertz techniques are applied to inspect the paint thickness by measuring the time delay of the reflected or transmitted terahertz waves induced on the paint layers. The terahertz technique can measure the multi-layer paint with 100  $\mu\text{m}$  of resolution, but the bulky and expensive experimental equipment are required for micro-level paint thickness estimation.

As alternative, an infrared (IR) thermography techniques are gaining its popularity as the non-contact paint thickness estimation by analysing the thermal waves propagating through the paint layers. Mezghani et al proposes a laser thermography system to inspect a paint thickness in a single point with a non-contact manner [1]. However, numerous time is required to visualize paint thickness distribution in wide area with integrating test results acquired from the multiple inspections. Shrestha and Kim shows an applicability of halogen thermography system as visualizing a paint thickness distribution through the numerical simulations to tackle the technical hurdles comes from the point inspection [2]. However, an actual halogen lamp cannot generate an even energy-leveled heat source on the large area and an inaccurate results can be occurred. Moreover, quite bulky volume of the halogen lamp can prevent its application to various fields.

To effectively inspect the thickness of the paint layer in the metallic structures, a laser scanning thermography (LST) system is proposed. The LST system can visualize the paint thickness distribution by analyzing the thermal waves propagating phenomena. The LST system has the following uniqueness: (1) The paint thickness distributions through the large area can be visualised; (2) The paint thickness can be not only visualized but also quantified without using any baseline data through the various external temperature conditions; (3) The paint thickness inspection is performed in a non-contact manner. The robustness and practicality of the proposed LST system is demonstrated using the actual test data obtained from an epoxy coated steel plate under varying exterior temperature conditions, with quantifying and visualizing the paint thickness distributions within 40  $\mu\text{m}$  of resolution.

The remainder of the paper is organized as follows. Section 2 describes the hardware configuration and working principles of the LST system. Further, an instantaneous paint thickness visualization algorithm is proposed in section 3. In section 4, the performance of the proposed LST system is validated experimentally using test data that is obtained from a painted steel plate under the various temperature conditions. Finally, the summary and discussion of our study concludes our research in section 5.



## 2. Development of the Laser Scanning Thermography (LST) System

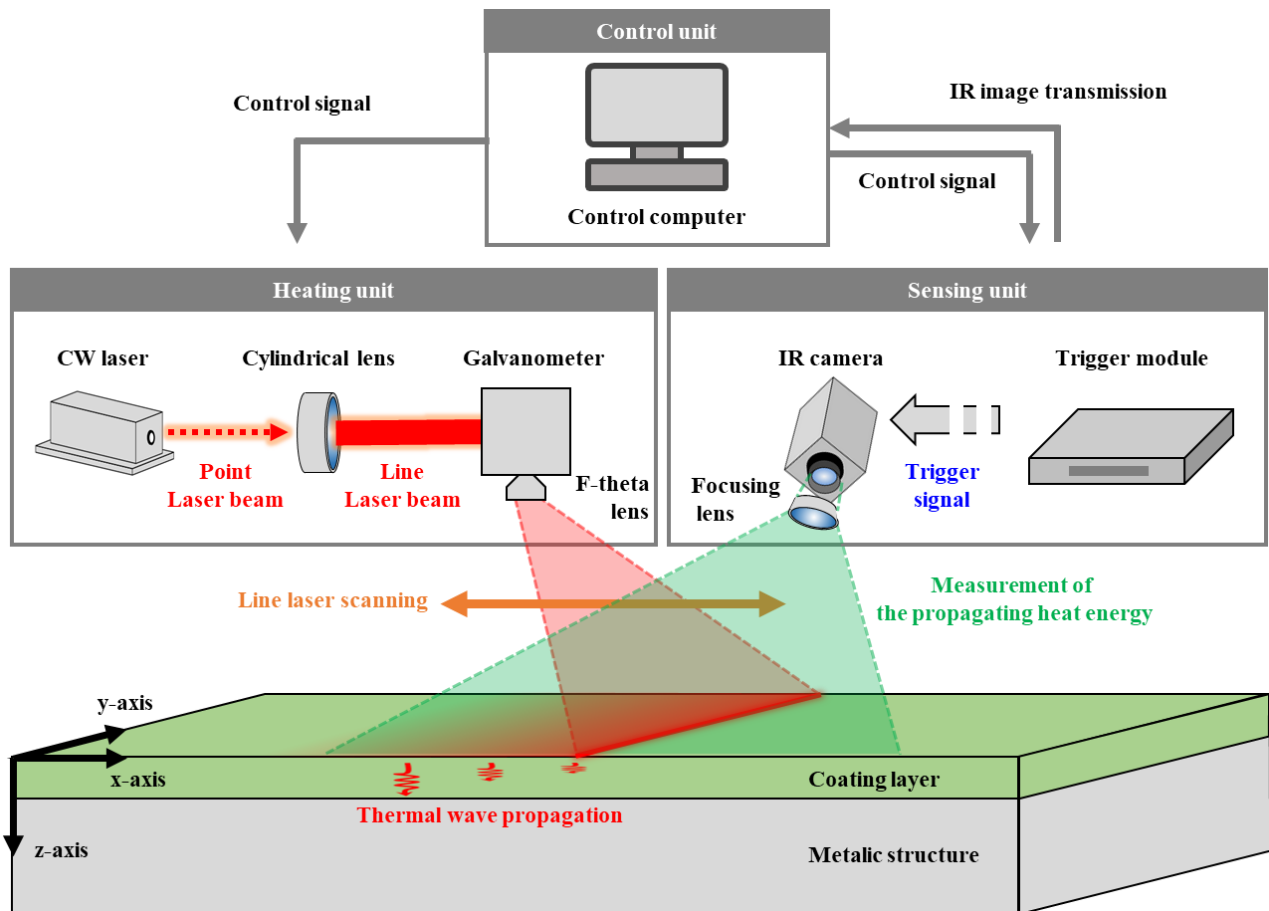
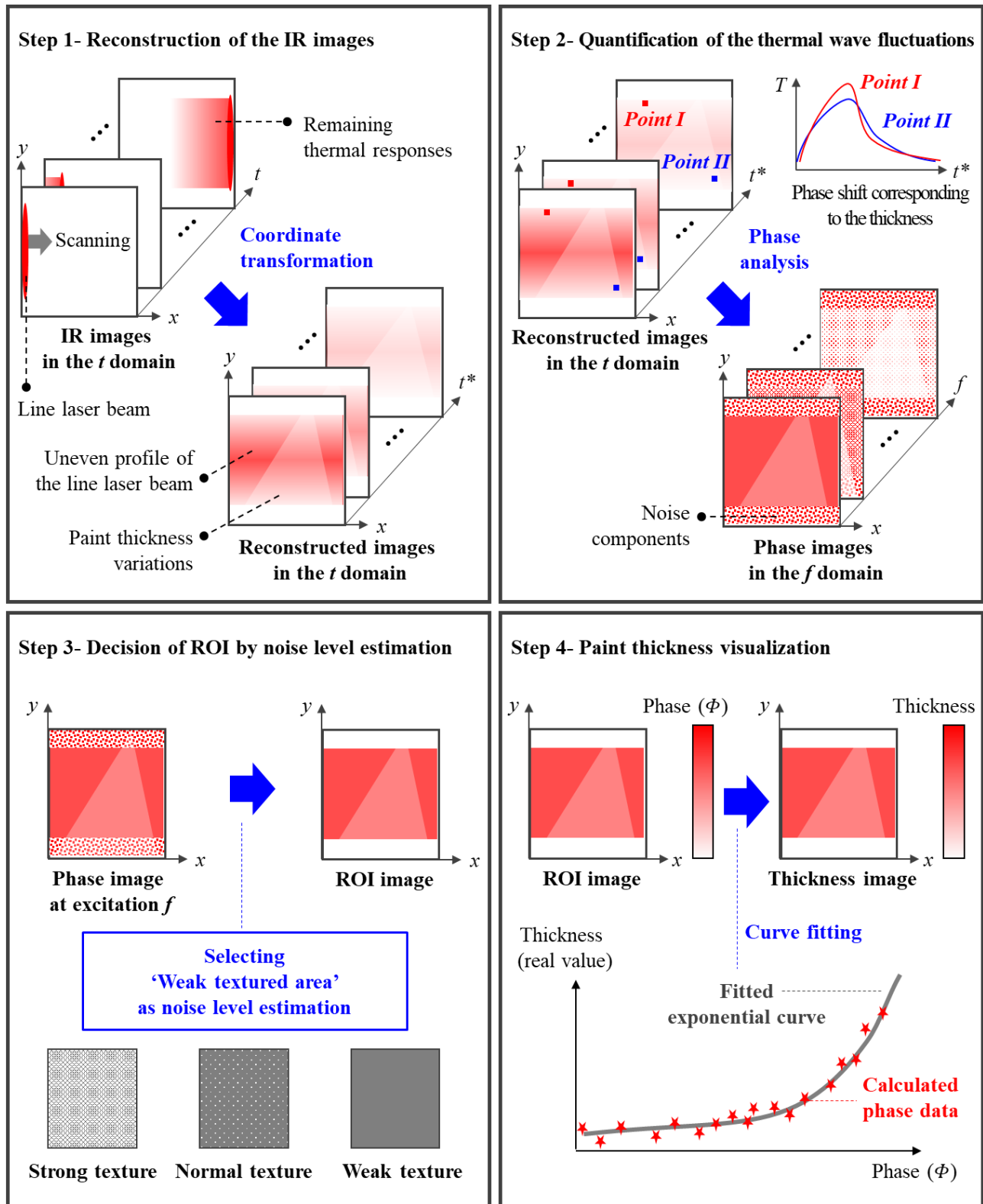


Fig. 1. Schematic representation of the laser scanning thermography (LST) system

The LST system is composed of three units: heating, sensing and control units, as shown in Fig. 1. The heating unit generates thermal waves to the target structure and is composed of a continuous-wave (CW) laser, a cylindrical lens, a galvanometer and an F-theta lens. The F-theta lens is mounted in front of the galvanometer. The sensing unit measures the thermal wave radiating through the target structure surface and is comprised of a trigger module, an IR camera, and a focusing lens. The control unit controls the heating and sensing unit and analyse the thermal waves measured from the sensing unit and is comprised of a control computer used to synchronize each unit by sending out control signals.

The working principles of the LST system is described as follows. First, the control unit sends out the control signals to the CW laser. Then the CW laser is activated and emits the point laser beam. The emitted point laser beam passes through the cylindrical lens. Then the shape of the point laser beam is transformed to the line laser beam that has the Gaussian profile in longitudinal directions ( $y$ -axis). Simultaneously, the control unit sends out the control signals to the galvanometer, and the line laser beam scans the paint layer surface continuously. Here, the F-theta is used to focus the line laser beam to the surface of paint layer and to prevent the shape distortion of the line laser beam. Then, the thermal waves are generated on the paint layer and propagate through the thickness directions ( $z$ -axis). Generally, the thermal waves are not able to propagate long distance in paint layers due to the low thermal conductivity (typically  $0.35 \text{ W m}^{-1} \text{ K}^{-1}$  for epoxy material and  $0.03 \text{ W m}^{-1} \text{ K}^{-1}$  for polyurethane material, which are widely used as paint layers). Thus, the resultant thermal waves on each spatial points of the paint layers show as if a short pulse laser beam is excited after continuously scanning the line laser beam in the orthogonal directions with the line laser beam ( $x$ -axis). Note that, the thermal wave propagating phenomena, such as amplitude and phase shift of surface temperature during heating and cooling process, differs corresponding to the paint thickness. The corresponding thermal responses are captured in the time and spatial domains by the IR camera after triggered by the trigger module in the sensing unit. Here, the inspection area and the working distance can be adjusted using the focusing lens. The captured thermal responses are transmitted to the control computer in control unit and stored as an IR images. The IR images are then processed using the proposed instantaneous paint thickness visualization algorithm in the control computer, simultaneously. The data acquisition and processing are performed automatically by LabVIEW® and MATLAB® programs installed in the control computer.

## 3. Development of the paint thickness visualization algorithm



**Fig. 2.** Overview of the paint thickness visualization algorithm: Step 1- Reconstruction of the infrared (IR) images, Step 2- Quantification of the thermal wave fluctuations, Step 3- Decision of region of interest (ROI) by noise level estimation, and Step 4- Paint thickness visualization

The thermal responses captured as IR image through the LST system is analysed to visualize and quantify the paint thickness distribution. The paint thickness visualization algorithm is processed through the following steps: step 1 – reconstruction of the IR images, step 2 – quantification of the thermal wave fluctuations, step 3 – decision of region of interest (ROI) by noise level estimation, and step 4 – paint thickness visualization. The details of each step is described as follows.

### Step 1 - Reconstruction of the IR image

The IR images acquired from the LST system are reconstructed by re-arranging time ( $t$ ) domain signal of each pixel on IR images as the reconstructed time ( $t^*$ ) domain signal of each pixel on reconstructed images based on the Equation (1):

$$I(x, y, t^*) = R(x, y, t - x/v) \quad (1)$$

where,  $I$  and  $R$  are the IR images and reconstructed images, respectively, and  $v$  is a scanning speed of the line laser beam. Note that the reconstructed image before the line laser beam starts heating the paint layer ( $t^* < 0$ ) is ignored. Instead of presenting a line laser beam with scanning along  $x$ -axis, the reconstructed images show the thermal responses as if a short pulse beam is excited on the whole measuring area. Here, the pulse width ( $\tau$ ) can be assumed using  $v$  and the width ( $w$ ) of the line laser beam as follows:

$$\tau = w/v \quad (2)$$

### Step 2 - Quantification of the thermal wave fluctuations

The reconstructed image cannot clearly visualize the paint thickness distribution. Because the temperature distributions on the paint layer can be spatially fluctuated by heat from line laser beam before and after the experiment due to (1) the ambient external temperature conditions; and (2) the uneven profile of the line laser beam. The temperature abnormalities on the paint layer caused by ambient external temperature conditions can be ignored by only considering the changes of phase angle and amplitude of thermal waves induced by the line laser beam [15]. However, temperature abnormalities on the paint layer due to uneven profile of the line laser beam cause the uneven amplitude changes since it has the same thickness of the paint layers. Thus, by estimating the paint thickness based on analyzing the phase changes, the uneven laser profile can be compensated. The phase delay ( $\Phi_n$ ) can be calculated using the discrete Fourier transform as follows:

$$F_n = \Delta t \sum_{k=0}^{N-1} T(k \Delta t) \exp^{i2\pi nk} = Re_n + Im_n \quad (3)$$

$$\Phi_n = \tan^{-1}(Im_n / Re_n) \quad (4)$$

where,  $i$  is the imaginary number,  $Re$  and  $Im$  are respectively the real and the imaginary parts of the transform.  $\Delta t$  is the sampling interval,  $n$  is the frequency increment ( $n=0, 1, \dots, N$ ).  $T$  is the surface temperature denoted by each pixel value on the IR images. After calculating  $\Phi_n$  for each spatial point of IR images, the paint thickness can be visualized nothing to do with the external temperature and laser profile. Here,  $n$  is selected the nearest natural numbered frequency calculated based on  $\tau$ .

### Step 3 - Decision of ROI by noise level estimation

A patch-based noise level estimation algorithm is used to find the noisy area on the phase image which has a strong texture based on the principal component analysis [16]. The area where the energy injection of line laser beam is not enough to generate the thermal energy to show strong textured pattern in the phase image as noise components. Thus, the region of interest (ROI) is constructed by eliminating the strong texture area on the phase image.

### Step 4 - Paint thickness quantification

Once the ROI image is constructed, the paint thickness quantification step is performed. An empirical mapping function is used to relate the thickness measured by eddy-current testing as a point inspection (MP0R-FP, Helmut Fischer GmbH) corresponding the various materials and color of the paint layer. An exponential regression is then performed to approximate the mapping function using the phase angle calculated by the experiment data and measured paint thickness. Once the empirical mapping function is trained, the phase angle is used as an input and the final paint thickness is calculated from the trained empirical mapping function as an output.

#### 4. Experimental validations

##### 4.1. Descriptions of test setup with target structures

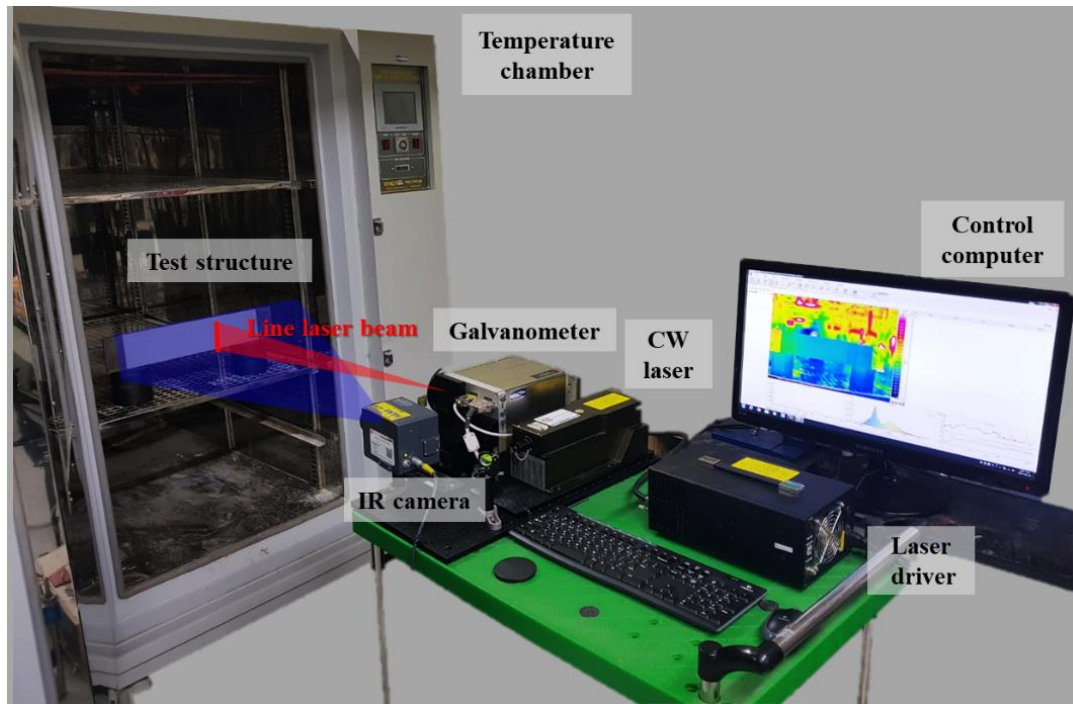
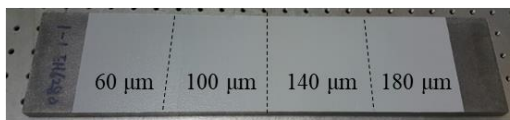
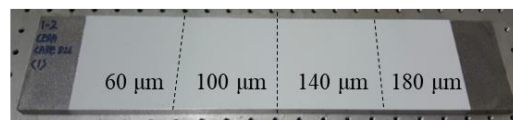


**Fig. 3.** Test setup for the validations of LST system

- Different types of materials but same color of coating layer

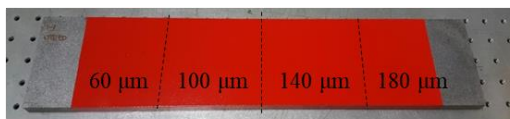


(a)

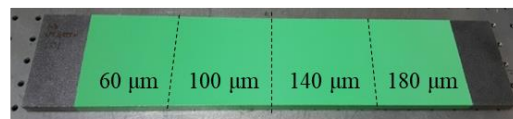


(b)

- Same type of materials but different colors of coating layer



(c)



(d)

**Fig. 4.** Steel plate structures with paint layer: paint layer of (a) epoxy material with grey color, (b) ceramic material with grey color, (c) urethane material with red color, and (d) urethane material with light green color.

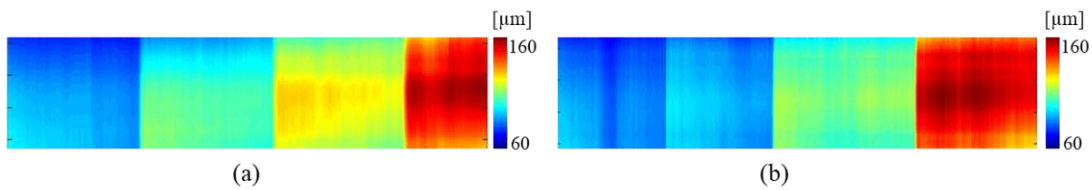
Fig. 3 shows the test setup for the validations of the proposed LST system, and Fig. 4 shows the target steel plates with paint layer used for the validation tests. Each steel plates has width 500 mm, height 100 mm, and thickness 12 mm of dimensions, and the each paint layer is coated with following materials: Fig. 4 (a)- epoxy material with grey color (EH6280, KCC Co., Ltd.); Fig. 4 (b)- ceramic material with grey color (CERACARE826, KCC Co., Ltd.); Fig. 4 (c)- urethane material with red color (UT6581, KCC Co., Ltd.); Fig. 4 (d)- urethane material with light green color (UT2578, KCC Co., Ltd.). As for the test setup and parameters, first, the control computer sends out the trigger and control signals to the CW laser, and the CW laser (TMA-532-15T, TMA) generates a point laser beam with 4 mm diameter and a 532 nm of wavelength. Here, the laser beam intensity is set to 92.31 mW/mm<sup>2</sup> considering the thermal conductivity of the test structure. The point laser beam is transformed into the line laser beam (100×1.3 mm<sup>2</sup>) using the cylindrical lens (CVI optics co., Ltd.). The line laser beam scans target structure and generates thermal waves with a constant scanning speed of 20 mm/s. The corresponding thermal responses are measured in  $t$  domain using the IR camera (VarioCam HiRes 640, InfraTec GmbH)

triggered by trigger module controlled by the control unit. The IR camera acquires IR images with a temperature resolution of 0.03 K, a sampling rate of 50 Hz, a spectral range of 7.5  $\mu\text{m}$  to 13  $\mu\text{m}$ , and spatial resolution of 780  $\mu\text{m}$ . The galvanometer and IR camera are 1000 mm apart from the target structure by considering the focusing length of the F-theta lens. The temperature of the test structure is controlled from -15  $^{\circ}\text{C}$  to 50  $^{\circ}\text{C}$  at 5  $^{\circ}\text{C}$  of intervals using the temperature chamber (EN-TH-1370, ENEX Scientific Industrial Co., Ltd.).

#### 4.2. Test results

The performance of the proposed LST system and the paint thickness visualization algorithm is validated using 4 coated steel plates which has 40  $\mu\text{m}$  of paint thickness difference per each area as shown in Fig. 4 and paint thickness is successfully visualized as shown in Fig. 5. Moreover, the chart described in Fig. 6 shows that the calculated phase angle corresponding to the paint thickness is nothing to do with the external temperatures.

- **Different types of materials but same color of coating layer**



- **Same type of materials but different colors of coating layer**

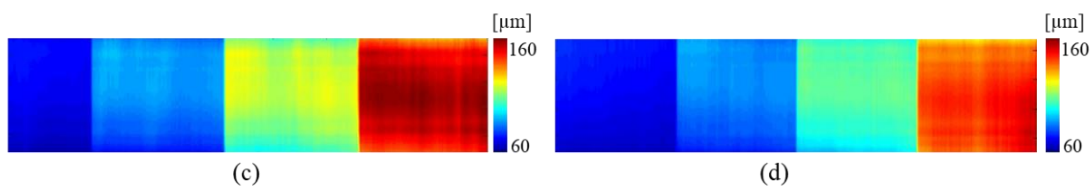


**Fig. 5.** Thickness image acquired from the target structure in 15  $^{\circ}\text{C}$  of initial temperature: paint layer of (a) epoxy material with grey color, (b) ceramic material with grey color, (c) urethane material with red color, and (d) urethane material with light green color

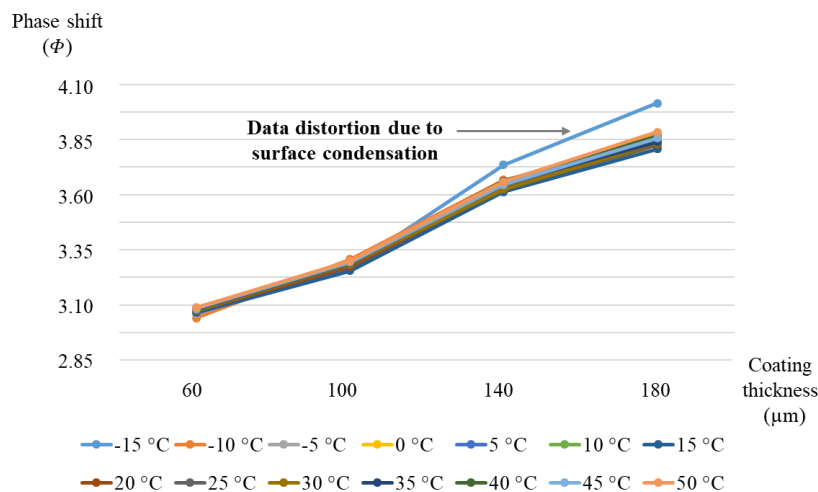


**Fig. 6.** Phase shift corresponding to the paint thickness under various initial temperature conditions of the target structure

#### 5. Conclusion

A laser scanning thermography (LST) system is proposed to visualize the paint thickness in noncontact manner. The main uniqueness of the proposed LST system is that it can rapidly and automatically visualize the paint thickness nothing to do with the exterior temperature conditions without using any baseline data. The verification test revealed that the proposed LST system can visualize and quantify the paint thickness with 40  $\mu\text{m}$  of resolution.

### ACKNOWLEDGEMENTS

This research was supported by a grant (18SCIP-C116873-03) from Construction Technology Research Program funded by Ministry of Land, Infrastructure and Transport of Korean government

### REFERENCES

- [1] Mezghani S, Perrin E, Vrabie V, Bodnar J, Marthe J, Cauwe B. Evaluation of paint thickness variations based on pulsed Infrared thermography laser technique. *Infrared Physics & Technology*. 2016;76:393-401.
- [2] Shrestha R, Kim W. Evaluation of paint thickness by thermal wave imaging: A comparative study of pulsed and lock-in infrared thermography–Part I: Simulation. *Infrared Physics & Technology*. 2017;83:124-31.
- [3] Zhang J-Y, Meng X-b, Ma Y-c. A new measurement method of paints thickness based on lock-in thermography. *Infrared Physics & Technology*. 2016;76:655-60.
- [4] Cha SC, Erdemir A. *Paint Technology for Vehicle Applications*: Springer; 2015.
- [5] Mezghani S, Zahouani H, Piezanowski J. Multiscale effect of paint pulverization orientation on appearance after painting. *Journal of Physics: Conference Series*: IOP Publishing; 2011. p. 012026.
- [6] Kayser JR, Nowak AS. Reliability of corroded steel girder bridges. *Structural Safety*. 1989;6:53-63.
- [7] Czarnecki AA, Nowak AS. Time-variant reliability profiles for steel girder bridges. *Structural Safety*. 2008;30:49-64.
- [8] Guo T, Chen Y-W. Field stress/displacement monitoring and fatigue reliability assessment of retrofitted steel bridge details. *Engineering Failure Analysis*. 2011;18:354-63.
- [9] Salem H, Helmy H. Numerical investigation of collapse of the Minnesota I-35W bridge. *Engineering Structures*. 2014;59:635-45.
- [10] Salem H, Helmy H, Fouly AE. Prediction of bridge behavior through failure: a case study of the Minnesota I-35W bridge collapse. *Structures Congress 2013: Bridging Your Passion with Your Profession* 2013. p. 2904-15.
- [11] García-Martín J, Gómez-Gil J, Vázquez-Sánchez E. Non-destructive techniques based on eddy current testing. *Sensors*. 2011;11:2525-65.
- [12] Fan M, Cao B, Tian G, Ye B, Li W. Thickness measurement using liftoff point of intersection in pulsed eddy current responses for elimination of liftoff effect. *Sensors and Actuators A: Physical*. 2016;251:66-74.
- [13] Zhao Y, Lin L, Li X, Lei M. Simultaneous determination of the paint thickness and its longitudinal velocity by ultrasonic nondestructive method. *NDT & E International*. 2010;43:579-85.
- [14] Koch FJ, Vandervalk LC, Beamish DJ. High resolution ultrasonic paint thickness gauge. *Google Patents*; 1998.
- [15] Ibarra-Castaneda C, Maldague X. Pulsed phase thermography reviewed. *Quantitative Infrared Thermography Journal*. 2004;1:47-70.
- [16] Liu X, Tanaka M, Okutomi M. Noise level estimation using weak textured patches of a single noisy image. *Image Processing (ICIP), 2012 19th IEEE International Conference on: IEEE*; 2012. p. 665-8.